DOI: 10.1002/cmdc.200600263

The Novel Antimalarial Compound Dioncophylline C Forms a Complex with Heme in Solution

Kai F. Schwedhelm,[a] Martin Horstmann,[a] Johan H. Faber,[b] Yana Reichert,[b] Gerhard Bringmann,[b] and Cornelius Faber*[a]

A structural model of the complex formed between the novel antimalarial compound dioncophylline C (DioC) and its presumed target ferriprotoporphyrin IX heme (FPIX) is presented. The complex structure was calculated with molecular dynamics (MD) simulations using intermolecular distance restraints between DioC and the iron center in FPIX, determined from NMR paramagnetic relaxation. Besides the spin state of the iron and longitudinal relaxation rates of hydrogen nuclei in DioC, the effective correlation time of paramagnetic relaxation was determined from NMR measurements at three different magnetic field strengths. The derived structural model shows high similarity to complexes formed by FPIX and antimalarials of the quinoline family (chloroquine, quinine, quinidine, and amodiaquine). The conformation of DioC is sterically stabilized by a water molecule coordinated to iron in FPIX. This structural feature may provide an important hint at possibilities for a further optimization of novel naphthylisoquinoline alkaloid (NIQ) antimalarial drugs.

Introduction

Malaria is an infectious disease causing more than 500 million incidences and 1.3 million death cases[1] every year, mainly in sub-saharan Africa. The cheapest and most commonly used antimalarial drug is chloroquine (CQ),[2,3] but adverse reactions by a large number of patients[4] and growing resistance of the most dangerous malarial parasite *Plasmodium falciparum*[5] to all drugs available (including mefloquine, doxycycline, atovaquone, and CQ)[6] make an investigation of the mode of action and the mechanism of resistance a major issue.

During the blood stage of the malaria infection, the parasite enters the erythrocytes and digests their hemoglobin. The released ferriprotoporphyrin IX heme (FPIX), which is noxious to the parasite,[2] is converted into its crystalline form, hemozoin,[7] which is nontoxic to *P. falciparum* and appears as dark black spots in the red blood cells of infected patients. In aqueous solutions, FPIX predominately forms a μ-oxo dimer, which consists of two FPIX monomers bridged by an Fe–O–Fe bond.[8,9] It has become increasingly evident that the mode of action of most antimalarial drugs is to interfere with hemozoin formation inside the digestive vacuole of the parasite.[10–14] The exact interaction between FPIX and drug molecules, and the resulting mechanism of action, however, are not yet completely understood, calling for a detailed investigation of the respective processes at a molecular level.

The interactions of FPIX with antimalarial drugs have so far been studied by applying a large variety of methods,[15–17] including paramagnetic NMR spectroscopy, a valuable source for structural information.[18–20] De Dios and co-workers have determined the first atomic resolution structures of FPIX in complex with several antimalarial drugs by NMR spectroscopy,[18] establishing a 2:1 stoichiometry of the FPIX:drug complexes and suggesting a possible role of the CQ side chain in stabilizing the complex. The strategy used in that and further NMR investigations, involved experimental determination of relaxation rates and spin states and relied on the assumption that a single conformation of the complex dominates in solution.[18,21,22] The calculated structures, therefore, represent the most stable, predominant conformation. Similar to structures determined by crystallography, no structural information on association intermediates is provided.

Herein, we follow the same approach and additionally determine the effective correlation time of paramagnetic relaxation to investigate the interaction of FPIX with the novel antimalarial drug dioncophylline C (DioC; the structure is depicted in Figure 1).[23,24] DioC shows a very low IC_{50} value of 0.0063 $\mu g\,mL^{-1}$ against *P. falciparum*, even in chloroquine-resistant strains, and low cytotoxicity.[25] The drug belongs to the family of the naphthylisoquinoline (NIQ) alkaloids and is found in the roots of the tropical liana *Triphyophyllum peltatum*.[23] Ex-

[a] *K. F. Schwedhelm, Dr. M. Horstmann, Dr. C. Faber*
Department of Experimental Physics 5
University of Würzburg
Am Hubland, 97074 Würzburg (Germany)
Fax: (+49) 931-888-5851
E-mail: faber@physik.uni-wuerzburg.de

[b] *J. H. Faber, Y. Reichert, Prof. Dr. G. Bringmann*
Institute of Organic Chemistry
University of Würzburg
Am Hubland, 97074 Würzburg (Germany)

Supporting information for this article is available on the WWW under http://www.chemeurj.org/or from the author.

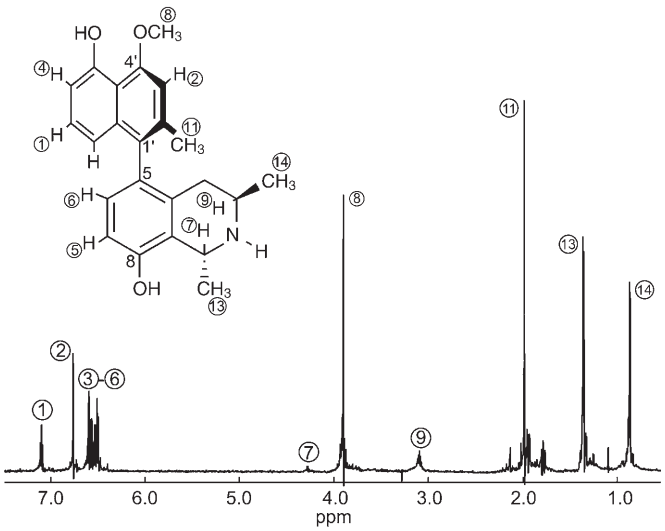

Figure 1. 1D ^{1}H NMR spectrum (2 mM) and chemical structure of dioncophylline C: H atoms are labeled sequentially according to their signal position in the NMR spectrum. This labeling scheme is also used for H atom identification in the MD simulations. Multiple appearance of a numeral indicates identical chemical shifts of the related H atoms.

tracts from this plant are commonly used in traditional African medicine for the treatment of severe tropical diseases including malaria.[24] It has been shown to be able to heal mice infected with *Plasmodium berghei* because of its good in vivo activity.[25]

Theoretical Background

FPIX has a paramagnetic iron atom situated at its center, which renders conventional NMR spectroscopy experiments for molecular structure determination impossible. Still, one can derive structural information by measuring the influence of the paramagnetic metal center on longitudinal relaxation times of nearby hydrogen atom spins.[18,26,27] The distance of each proton in the drug molecule from the paramagnetic center can be related to its longitudinal relaxation rate by the Solomon-Bloembergen equation:[28]

$$r = \left(\frac{2}{15}\left(\frac{\mu_0}{4\pi}\right)^2 \frac{\hbar^2\gamma_I^2\gamma_S^2 S(S+1)}{R_{\text{complex}}}\left(\frac{\tau_C}{1+(\omega_S-\omega_I)^2\tau_C^2}+\frac{3\tau_C}{1+\omega_I^2\tau_C^2}+\frac{6\tau_C}{1+(\omega_S+\omega_I)^2\tau_C^2}\right)\right)^{\frac{1}{6}} \quad (1)$$

where R_{complex} is the longitudinal relaxation rate of the nuclear spin in the complex, r is the distance between the paramagnetic center and the observed H atom, S is the electronic spin state of Fe, τ_C is the effective correlation time, ω_I is the proton Larmor frequency, and $\omega_S = 658\,\omega_I$ is the electron Larmor frequency. μ_0 is the magnetic permeability of vacuum, $\hbar$ is Dirac's constant, and γ_I and γ_S are the gyromagnetic ratios of the nucleus and the electron.

The spin state S can be determined using a method proposed by Evans.[26,29,30] The chemical shift of any given H atom resonance in the spectrum depends on the bulk susceptibility χ_0 of the surrounding medium. The susceptibility is related to the effective number of unpaired electrons and, thus, the spin state of the paramagnetic metal in the sample. By comparing NMR resonance frequencies of a reference solution with samples containing the paramagnetic compound, the spin state of the paramagnetic element can be derived. R_{complex} can be measured by standard inversion recovery experiments using the pulse sequence 180°-τ-90°. The effective correlation time can be derived from experiments at multiple B_0 fields using Equation (1).

Determination of Effective Correlation Times

The effective correlation time τ_C is a time constant describing fluctuating magnetic fields that lead to relaxation of nuclear spins in the drug molecule. τ_C is composed of the correlation time for electron spin relaxation τ_S, the rotational correlation time τ_r, and the correlation time for chemical exchange τ_M:[26]

$$\frac{1}{\tau_C} = \frac{1}{\tau_S} + \frac{1}{\tau_r} + \frac{1}{\tau_M} \quad (2)$$

τ_r can be approximated from the Stokes-Einstein equation. For the FPIX:DioC complex it can be expected in the range of 10^{-9} s. τ_M can be estimated from the dissociation constant of the complex. Assuming that the association rate is diffusion limited, τ_M can be approximated to be larger than 10^{-9} s. The electronic correlation time τ_S is usually in the range of 10^{-13} s to 10^{-10} s.[26] Therefore, it is not a priori clear that τ_C will be dominated by τ_S and thus, has to be determined experimentally. This can be done if two assumptions are made:

1. The intermolecular distances in the FPIX:DioC complex are independent of the applied magnetic field.
2. τ_C does not change significantly with the applied magnetic field.

As R_{complex} and the Larmor frequencies are the only quantities in Equation (1) that depend on B_0, it is possible to derive the effective correlation time τ_C for every H atom resolved in NMR spectra acquired at different magnetic fields. Fitting Equation (1) as a function of the Larmor frequency to the relaxation rates R_{complex} determined at different field strengths, yields τ_C as a fit parameter.

Materials and Methods

Ferriprotoporphyrin IX chloride (FPIX), 2,2,6,6-tetramethylpiperidine 1-oxyl (TEMPO), 3-(trimethylsilyl)propionic acid-d_4 sodium salt (TSP), phosphate buffered saline (PBS), 5 mm NMR tubes, and WILMAD coaxial inserts were purchased from Sigma–Aldrich Chemie GmbH (Munich, Germany). Deuterium oxide (D_2O) and deuterium sodium oxide (NaOD) were obtained from Euroisotop (Saarbrücken, Germany). Dioncophylline C (DioC) was isolated from *Triphyophyllum peltatum* and purified (purity > 98 %, according to ^{1}H NMR) as published previously.[23]

Sample Preparation

For the UV experiments, stock solutions of FPIX were prepared daily by dissolving hemin chloride in 10 mM NaOH in a concentration of 1.68 mM and subsequently diluted with H_2O PBS (10 mM, pH 6.5) or with H_2O, to give a final concentration of 0.168 mM. Stock solutions of DioC were prepared in a concentration of 0.168 mM in H_2O buffered with PBS (10 mM, pH 6.5) or H_2O adjusted to pH 11 using 10 mM NaOH.

For NMR spectroscopy relaxation rate measurements, stock solutions (10 mM) of DioC in D_2O and of FPIX (15.0 mM) in 50 mM NaOD were prepared in Eppendorf tubes and used within 60 min. Aliquots of the DioC and FPIX stock solutions were mixed in predetermined ratios to give a final concentration of 2.0 mM dioncophylline C and 0–0.2 mM FPIX. The samples were diluted using D_2O and 10 mM NaOD to give a final sample volume of 800 μL and an adjusted pD of 11. The samples were subsequently transferred into 5 mm NMR tubes. FPIX:DioC samples with pD values below 11 were not sufficiently stable for the NMR spectroscopy experiments.

UV Spectroscopy

UV spectroscopy was performed on a Varian Cary 50 spectrophotometer (Varian, Varian, Inc., Palo Alto, CA, USA). The absorbance was measured at 365 nm with standard 1 cm cuvettes, requiring a sample volume of 1.5 mL.

For determination of the binding stoichiometry between FPIX and DioC, Job's plot analysis was used.[31,32] The complex formation-dependent changes of the UV absorbance at $\lambda =$ 365 nm were analyzed. Test solutions of 0, 0.105, 0.21, 0.315, 0.42, 0.525, 0.5775, 0.63, 0.6825, 0.735, 0.7875, 0.84, 0.8925, 0.945, 1.05, 1.155, 1.26, 1.365, 1.47, 1.575, 1.68, 1.785, 1.89, 1.995, and 2.1 mL of the 0.168 mM DioC stock solution (pH 6.5 and pH 11) were adjusted to a final volume (V_T) of 2.1 mL by the addition of the 0.168 mM FPIX stock solution.

For determination of the binding constant, titrations of 2 mL of the FPIX solution with the DioC stock solutions (pH 6.5 and pH 11) were monitored by the decrease of the UV absorbance at $\lambda = 365$ nm. The volume of titration steps was 10 μL and the relative molar ratio was varied between zero and eight with respect to FPIX. Spectra were recorded about 10 min after each addition. Difference absorption spectra derived from the titration ranged in intensity from ≥ 0.01 a.u. to ≤ 0.08 a.u. Digested titration data were corrected for dilution and the corresponding binding isotherm was analyzed using a nonlinear curve fitting model with a 1:1 association model (FPIX-μ-oxo dimer:DioC).[32]

NMR Spectroscopy

1D ^{1}H NMR spectra for Fe spin state determination were acquired on a Bruker DMX 600 (14.1 T) spectrometer. A coaxial NMR tube system (WILMAD, Wilmad-LabGlass, Buena, NJ, USA) was used. The inner capillary contained 100 μL of a 1 mM TSP solution in D_2O with PBS (10 mM, pD 11) in all experiments in aqueous solution. For determination of the geometry factor the outer capillary contained 1 mM TSP and the standard radical molecule TEMPO in a concentration of 2 mM. For the actual spin state determination experiments, aliquots of the aqueous stock solutions of FPIX and of DioC were mixed in Eppendorf tubes to give a concentration in the final sample of 1.0 mM FPIX (dimer) and predetermined titration steps of DioC in the range of 0–8 molar equivalents. A stock solution of TSP in D_2O (100 mM) was prepared, and aliquots thereof were added to the samples to give a final concentration of 1 mM TSP. A solution of D_2O with PBS (10 mM, pD 11) was added to give a total sample volume of 500 μL. Argon was gently bubbled through the samples for 30 min. to eliminate paramagnetic oxygen impurities. Subsequently, 300 μL of the samples were transferred to the outer tube of a coaxial tube system. The frequency shift between the TSP resonance line in the outer tube containing FPIX and the reference solution in the inner capillary was plotted against the concentration of FPIX in the sample. Evaluation of the frequency shift between the water resonances in the sample and reference compartments yielded the same results. For calculation of the spin state, magnetic coupling between the two Fe ions was considered weak.[33]

For the determination of T_1 relaxation rates, ^{1}H NMR spectra of each sample were recorded on three different spectrometers (three different magnetic field strengths). FPIX:DioC (pD 11) was measured on Bruker Avance 400 (9.4 T), Bruker DMX 600 (14.1 T), and Bruker Avance 750WB (17.6 T) spectrometer (Bruker Biospin GmbH, Rheinstetten, Germany). Sample temperature was 299 K. Drug peaks of DioC were assigned as shown in Figure 1. No changes in drug chemical shifts were observed in any of the samples. FPIX resonances were strongly broadened and could not be assigned.

As a result of strong signal broadening caused by the paramagnetic metal center in FPIX, a direct investigation of the FPIX:drug 1:1 complex was not possible. This problem was overcome by a technique presented by Leed et al.:[18] In samples containing both free drug and drug bound to the iron-bearing molecule, line broadening is reduced if the free drug is in excess and the two species are in fast exchange. Under these conditions, the observed relaxation rate $R_{observed}$ is an average of the relaxation rate R_{free} of the free drug and the relaxation rate of the drug bound to FPIX, $R_{complex}$. Therefore, R_1 was determined from an NMR titration with a series of seven samples with increasing amounts of FPIX. The FPIX:drug ratios were 0:1, 1:100, 1:80, 1:60, 1:40, 1:20, and 1:10. The total drug concentration was held constant at 2 mM in all samples. T_1 values for each sample were determined using an inversion recovery pulse sequence with Watergate (W5)[34] water suppression to eliminate residual water signals. As a result of the increasing concentrations of FPIX, the paramagnetic effect on H atoms in the bound drug molecule likewise increased and their longitudinal relaxation times shortened. The relaxation rate $R_{complex}$ was derived by plotting the recorded values $R_{observed}$ against [FPIX]/(K_D+[drug]). The value of $R_{complex}$ was calculated for each resonance resolved in the spectra by extrapolating $R_{observed}$ by a linear fit to a 1:1 (FPIX-μ-oxo dimer:DioC) ratio.

The effective correlation time τ_C for each resonance was calculated by fitting Equation (1) to the relaxation rates obtained

from measurements at three different magnetic fields. The fitting procedures were performed using MATHEMATICA Version 5 (Wolfram Research, Champaign, IL, USA).

Molecular Modeling

Intermolecular distances between Fe in FPIX and individual H atoms in the drug molecule were obtained by evaluating the Solomon-Bloembergen equation, Equation (1), for every signal in the NMR spectrum. Following the approach by Leed et al.,[18] we assume the calculated distances to represent a single, lowest energy structure of the complex. Any conformational intermediates that may occur during complex formation or dissociation are assumed to have only negligible influence on the experimental data because of their short lifetimes as compared to the complex conformation. The calculated distances were used as constraints for molecular dynamics simulations of the complex using the XPLOR[35] software package. The Crystallographic Information File (CIF) of the FPIX-μ-oxo dimer was taken from the literature[8] and used as an initial structure. DioC was constructed using Chem3D Ultra software version 9 (CambridgeSoft, Cambridge, MA, USA). The 3D datasets were converted into pdb format and the corresponding XPLOR parameter and topology files were created using the "Hetero-Compound Information Centre - Uppsala" (HIC-Up) Server.[36] The FPIX monomer was also obtained from the HIC-Up Server. The database provides XPLOR parameters based on the standard CHARMM force field which are optimized for restrained structure refinement of small molecules.[37] The obtained parameters for DioC, the FPIX monomer, and the FPIX-μ-oxo dimer were combined and energy minimized, which provided the templates for the FPIX:DioC complexes. The initial template was then subjected to XPLOR simulated annealing (nmr/sa.inp) and simulated annealing refinement (nmr/refine.inp) protocols. Simulated annealing involved 200 000 steps at high temperature followed by cooling the system in 100 000 steps from the initial temperature of 2000 K. Simulated annealing refinement included a cooling period from 1000 K to 100 K in 200 000 steps. During both protocols, the intermolecular distances derived from the NMR spectroscopy data were included as distance restraints between the molecules. Deviations of 0.4 Å were allowed without penalty on the energy function. Distances to methyl groups were restrained to their center of mass. Distances obtained from degenerate resonances (signals 8, 11, 13, and 14 in DioC; see Figure 1) were used as restraints for every single H atom without additional tolerance.

For DioC and the FPIX-μ-oxo dimer a set of 400 structures was calculated. The resulting models were sorted by total energy. Structures with planarity, chirality, or bonding violations or those with deviations greater than 1.0 Å from the allowed distance restraints were discarded. Approximately 270 structures were accepted according to these requirements. Of this pool, 30 least-energy models were selected and overlaid and used for further analysis using the PyMOL software package.[38] For DioC with two FPIX monomers a set of 300 structures was calculated. Ambiguous distance restraints to both Fe atoms were introduced and averaged using the R-6 function[39] of XPLOR, which does not discriminate against longer distance values. Owing to the higher flexibility of the system, deviations of ± 2 Å were allowed. 139 structures were accepted according to the above criteria.

Results

Complex formation between FPIX and DioC was observed by UV spectroscopy. Job's plot analysis of the changes in the absorbance at 365 nm showed that a complex is formed with a molar ratio of two FPIX molecules per one DioC molecule (Figure 2). The 2:1 stoichiometry of the FPIX:DioC complex was

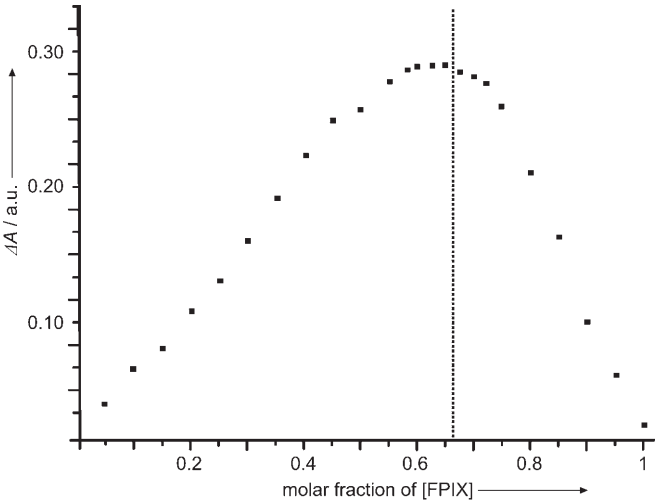

Figure 2. Job's plot of the complex dependent changes of the UV absorbance ΔA at 365 nm. Indicating the 2:1 stoichiometry of the FPIX:DioC complex formation. The molar fraction is given relative to FPIX.

found for both pH levels investigated (pH 6.5 and pH 11). The dissociation constants K_D for FPIX:DioC were determined as $(2.1 \pm 1.6) \times 10^{-5}$ M and $(2.5 \pm 1.2) \times 10^{-5}$ M at pH 6.5 and pH 11, respectively.

The spin state of the iron in FPIX was determined from measurements of the bulk susceptibility as a function of the relative amount of DioC added. No significant change in the number of free electrons per iron atom was observed upon addition of DioC. n remained nearly constant at approximately $n = 3.2$, indicating a spin state of $S = 3/2$ for the FPIX:drug complex.

The 1D ^{1}H NMR spectrum of DioC exhibited twelve signals, of which nine could be resolved and assigned in all samples (Figure 1). For each of the labeled signals, the relaxation rate $R_{complex}$ was derived. Figure 3 shows a representative plot of the measured relaxation rates R for all resonances over the concentration of FPIX [FPIX]/(K_d + [DioC]). The linear fits provide different slopes for each signal, indicating different influences of the paramagnetic Fe atom and thus different Fe–H distances. $R_{complex}$ was determined by extrapolating the curves shown in Figure 3 to a 1:1 ratio. Values of $R_{complex}$ obtained at the three different magnetic fields are summarized in Table 1.

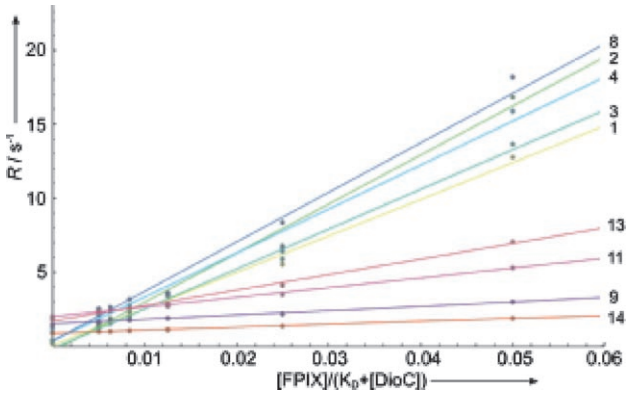

Figure 3. Determination of the relaxation rates: example plot of the longitudinal relaxation rate R at 750 MHz for all resonances (indicated on the right margin) in the spectrum versus the concentration of FPIX in the sample, [FPIX]/(K_D+[DioC]). [DioC] was held constant at 2 mM and [FPIX] was increased during the NMR titration. The paramagnetic effect causes R to increase with [FPIX]. No error bars are indicated, as each relaxation rate was determined with high precision. The main error source in the extrapolated relaxation rates is due to uncertainties of the concentration.

τ_C was derived by fitting the Solomon-Bloembergen equation, Equation (1), as a function of the proton Larmor frequency, to the experimentally derived values of $R_{complex}$. A representative plot of this procedure for $R_{complex}$ obtained for resonance 8 (see Figure 1) in FPIX:DioC at 400, 600, and 750 MHz is given as Supporting Information. The numerical two-parameter fit of the Solomon-Bloembergen equation (solid line) was performed independently for each of the resonances. Individual values for τ_C are listed in Table 1. The mean value of $(5.88\pm0.15)\cdot10^{-13}$ s was used for the calculation of all distance restraints. The procedure of performing a two-parameter fit with only three data points is critical. However, all individual values have moderate standard deviations and comply with the mean within one standard deviation, evidence that this procedure is reasonable. Further, the mean value is in the same order of magnitude as the value of 2×10^{-12} s, assumed in previous studies for the calculation of structures of complexes of FPIX with other antimalarial drugs.[18,21]

From the two global parameters (τ_C, S) and $R_{complex}$ for each resonance, intermolecular distances between the metal center in FPIX and the corresponding H atoms in the drug molecule were calculated with Equation (1). Distance restraints for the following molecular dynamics simulation were obtained from the mean values of a set of three distances, calculated for each of the different magnetic field strengths, for each individual resonance in the spectra (Table 1). The standard deviation from the mean value was always below 10% (< 0.4 Å). Major contribution to the experimental uncertainty, which was estimated to ±1 Å, resulted from uncertainties in the sample concentrations.

According to the observed 2:1 stoichiometry, there are two conceivable arrangements of the FPIX:DioC complex. Either DioC associates with the FPIX-μ-oxo dimer, or two FPIX monomers form a sandwich-like complex with DioC, similar to the structure proposed for quinine.[40] To account for both possibilities, MD calculations were performed with one DioC molecule and two FPIX monomers. Two possible overall conformations were observed. Details and illustrations of the resulting structures are provided as Supporting Information (Figure S2). Of the 300 calculated structures, 63 showed a sandwich-like complex. However, this arrangement is unlikely to reflect the structure in solution for three reasons. First, the position of the FPIX molecule on top is not unambiguously defined. Second, distances between the FPIX monomers and DioC are too large (> 7 Å) to allow for stabilizing interactions between the three molecules. Third, formation of a ternary complex implies a two-step association process as also proposed for quinine.[40] This can be ruled out for the FPIX:DioC system, because the relaxation rates show linear concentration dependences, clearly indicating second-order kinetics. 76 structures showed a different conformation with DioC positioned closely over one FPIX monomer, whereas the other monomer was found at large distances, not interacting with the binary complex (Supporting Information, Figure S2). This arrangement clearly contradicts the 2:1 stoichiometry. However, it reflects the interaction of DioC with one subunit of the FPIX-μ-oxo dimer as was shown in further MD simulations. In the calculated DioC:FPIX-μ-oxo dimer complex (Figure 4a and b), DioC is located above the central Fe atom in FPIX, but does not interact directly with the iron. Both the naphthyl and the isoquinoline moiety are tilted with respect to the FPIX tetrapyrrole. The included angles are 25 degrees for the naphthyl and 38 degrees for the isoquinoline moiety of DioC. This conformation of the drug leaves a void between the two molecules, which is sufficiently large to accommodate a water molecule. Therefore, the MD calculations were also performed with an H_2O molecule coordinated to

Table 1.
Calculated relaxation rates $R_{complex}$ of the FPIX:DioC complex.[a]

Atom	R/s^{-1} 400 MHz	R/s^{-1} 600 MHz	R/s^{-1} 750 MHz	τ_C [10^{-13} s]	Fe-H distance r [Å]		
					exp.	MD	MD + H_2O
1	109	78.7	55.4	5.96 ± 0.34	4.72	5.75	5.71
2	91.1	65.9	50.9	6.02 ± 0.26	4.83	5.70	5.71
3	79.0	59.9	47.4	5.95 ± 0.17	4.91	5.13	5.08
4	86.1	–	43.2	–	–	5.90	5.86
8	133	96.9	72.8	5.99 ± 0.28	4.54	5.14	5.16
9	–	32.6	33.8	–	–	4.72	4.73
11	52.0	39.4	27.4	5.86 ± 0.27	5.31	5.85	6.18
13	38.1	31.1	21.0	5.63 ± 0.19	5.56	6.44	6.47
14	73.5	58.6	38.8	5.72 ± 0.24	5.00	5.48	5.72

[a] At 9.4 T (400 MHz), 14.1 T (600 MHz), and 17.6 T (750 MHz) magnetic field strengths, Fe–H distances calculated with Equation (1), and distances derived from final structures calculated by molecular dynamics simulations. The mean value for τ_C is $(5.88\pm0.15)\times10^{-13}$ s. Resonances 4 at 600 MHz and 9 at 400 MHz were not resolved.

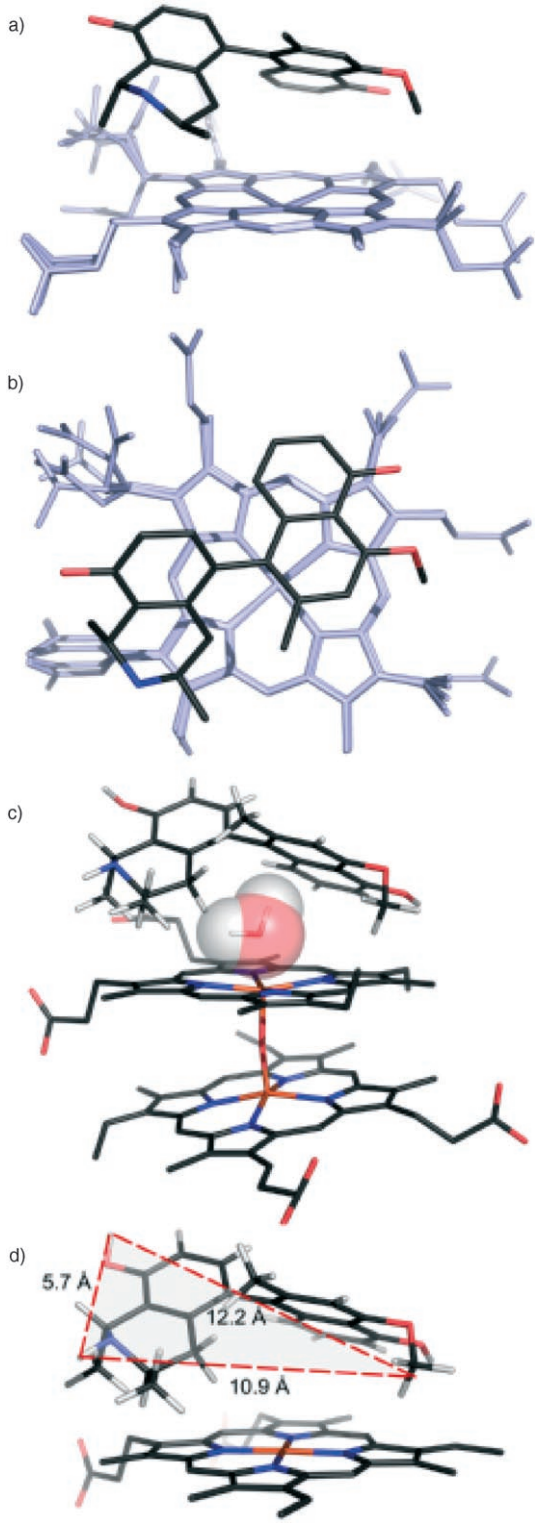

Figure 4. a) and b) Calculated structural model of the FPIX:DioC complex: for reasons of clarity, only seven of the 30 structures used for analysis are overlaid by superimposition of DioC. The water molecule between FPIX and DioC is not shown; c) Complete lowest energy structure calculated for the FPIX:DioC complex; d) Illustration of the triangular-shaped pharmacophore hypothesis: conformation of DioC is in agreement with distances predicted by 3D-QSAR[49] (see text).

the iron in the upper FPIX unit of the FPIX-μ-oxo dimer (Figure 4c). In the presence of the water molecule, calculated distances changed by less than 1% except for two methyl groups (resonances 11 and 14) where 5% larger distances to the iron center were obtained. The lowest energy of the FPIX:DioC complex was 452 kcal mol^{-1}, which is comparable to values reported for FPIX:quinine. FPIX:CQ and FPIX:quinidine showed higher energies of approximately 550 and 650 kcal mol^{-1}, respectively.[18] The FPIX:amodiaquine complex had remarkably lower energies (220 kcal mol^{-1}).[21]

No covalent or hydrogen bonding interactions were observed and the FPIX dimer rotated freely in multiples of 90° around its central axis. The structures give no evidence for an electrostatic interaction of the positively charged nitrogen in DioC with the negatively charged propionic acid side chains of FPIX, as the residing DioC does not have any obvious influence on the position of the FPIX side chains. This suggests a noncovalent stabilization of the complex, presumably through π-π-interactions of aromatic electron systems. Especially the naphthyl moiety of DioC is not located above the Fe center in FPIX, but occupies a position slightly shifted towards the edge of the FPIX tetrapyrrole, where favorable π-π-interactions to aromatic ring systems in FPIX are strongest. In this position, the closest proximity between DioC and the FPIX tetrapyrrole is 3.1 Å (C5′ in the naphthyl moiety of DioC) and increases to 5 Å (C2′). This spacing allows for attractive π-π-interactions between noncoplanar aromatic systems[41] which may be the largest contribution to complex stabilization. Similar orientations of aromatic moieties in drug molecules to the FPIX tetrapyrrole have been reported for quinoline-based antimalarials.[18,21] Moieties that are involved in π-π-interactions are always shifted towards the rim of FPIX and tilted by an angle between 20 and 40 degrees with respect to the FPIX tetrapyrrole. π-π-interactions are also possible in the isoquinoline moiety of DioC, however, because of a maximum distance of 5.7 Å (C6) to the FPIX tetrapyrrole, they have to be expected significantly weaker. The isoquinoline nitrogen is facing away from the iron center in FPIX, ruling out any possible direct interaction between these two atoms, as suggested previously for quinolines.[42]

Simulations conducted here, are the first to explicitly include a water molecule as a ligand to FPIX. Interestingly, we did not observe additional contributions to complex stabilization from hydrogen bonding or electrostatic interactions between the enclosed water molecule and DioC. The importance of water for complex formation was demonstrated by a set of identical experiments, carried out with FPIX and DioC in methanol, instead of D_2O. No changes in relaxation times of DioC were observed, indicating that no complex was formed between the two molecules. The role of the water molecule coordinated to the iron center is, presumably, the steric stabilization of the conformation of DioC. Relative rotations of the naphtyl and quinoline moiety around their C–C bond are restricted, thus preventing deviations from the orientation of most favorable π-π-interactions.

Discussion

The structural model of the FPIX:DioC complex shows an overall arrangement similar to complexes formed between FPIX and other drugs of the quinoline family like CQ, quinine (QN), quinidine (QD),[18] and amodiaquine (AQ).[21] Indications for covalent or hydrogen bonds between FPIX and the drug molecule were not observed in any of the complexes. For CQ, this finding is supported by electrospray-ionization mass spectroscopy[43] and polarization-resolved resonance Raman spectroscopy[44] on FPIX:CQ complexes. Both studies rule out a covalent interaction between the molecules. From these findings, the question arises how the complexes are stabilized. As shown previously,[45] a noncovalent interaction can consist of out-of-plane π-electrons in the drug and in the FPIX tetrapyrrole, capable of forming favorable π-π molecular recognition interactions. This enthalpy-driven process contributes to a stabilization of the complex. In recent theoretical calculations on π-π-interactions between benzene aromatic ring systems,[41] the strongest interaction was found for parallel-aligned rings at an interplanar distance of 3.5 Å. When the rings were not aligned parallel, the distance of highest attraction increased with the angle included between the rings. At an angle of 90 degrees, the highest attraction was found at about 5 Å intermolecular distance.[41] Theses values are in good agreement with the distances and angle between the FPIX tetrapyrrole and the naphthyl moiety of DioC, as reported here. Further stabilization of the complex may result from perturbed water molecules that are driven away from the hydrophobic surfaces of the molecules[46] during the alignment of DioC and FPIX. This assumption is supported by the finding that no complex was formed in methanol. For CQ, water was also found to be involved in complex formation, whereas other (organic) solvents weakened this interaction.[47]

The most obvious difference to complexes of other antimalarial drugs is the possible presence of a water molecule as a Fe ligand. A water molecule on the sixth coordination site of FPIX provides an explanation of the observed spin state of $S=3/2$. Common spin states for the FPIX monomer are $S=1/2$ (low spin) and $S=5/2$ (high spin). For the FPIX:CQ complex, $S=1/2$ was found at pH 6.5.[18] There are two possible conformations resulting in the $S=3/2$ spin state as reported here. First, antiferromagnetic coupling between the two iron centers in the FPIX-μ-oxo dimer might lead to an intermediate spin state of $S=3/2$ for both Fe atoms.[48] Second, the observed spin state might be an average between the iron centers in the FPIX-μ-oxo dimer, one in low spin and the other in high spin configuration. The spin state of Fe depends on the coordinated ligand. A water molecule (as enclosed between FPIX and DioC) acts as a weak ligand and therefore leaves the iron center in an $S=5/2$ (high spin) configuration. On the opposing side of the μ-oxo dimer, the iron center might be forced into a $S=1/2$ (low spin) configuration by a stronger ligand, such as OH^-. Such a stronger ligand might also be the propionic acid side chain of a second FPIX-μ-oxo dimer. However, higher adducts of FPIX do not comply with our data, except for a tetrameric DioC:FPIX-μ-oxo-dimer:FPIX-μ-oxo-dimer:DioC adduct that is still in agreement with the reported stoichiometry.

A common problem in structural investigations of FPIX in complex with quinolines[18,21] and with DioC, is that samples cannot be prepared at acidic pH values as found inside the digestive vacuole of the *Plasmodium* parasite. However, Leed et al.[18] were able to demonstrate that complexes of FPIX:CQ did not change significantly when calculated for different pH values. We found nearly identical K_D values for FPIX:DioC at pH 6.5 and pH 11. Both observations suggest that the association of these complexes is not strongly influenced by pH. We therefore assume that the structure of the FPIX:DioC complex presented here is a suitable model for the interaction of FPIX and DioC also at physiological pH in the digestive vacuole of the *Plasmodium* parasite.

The notion that the calculated structural model correctly reflects the biologically active conformation of DioC is further corroborated by the triangular-shaped pharmacophore hypothesis.[49] The 3D-QSAR technique MaP has previously been applied to characterize the antimalarial activity of various naphthylisoquinoline alkaloids. The study shows a specific geometric arrangement of three structural features in the drug molecule to be important for its biological activity: An unsubstituted nitrogen (for example, a secondary aminofunction) in position 2, a methoxy function at C4′, and a hydroxyl function at C8 (Figure 4d). In our structures (Figure 4a and b), the distances between these three features are 5.7 Å (NH-OH), 12.2 Å (OH-MeOH), and 10.9 Å (NH-MeOH), showing good agreement with the proposed 6–8 Å (NH-OH), 10–12 Å (OH-MeOH), and 12–14 Å (NH-MeOH), respectively.

The overall conformation of the FPIX:DioC complex is very similar to that suggested for the FPIX:CQ complex. Both drugs take a position above the FPIX tetrapyrrole and are slightly tilted with respect to FPIX. These similar structures hint at a similar mechanism of interferences with heme detoxification for DioC and CQ. Both drug molecules may inhibit hemozoin crystal formation by plasmodium by association with FPIX.[5,12] Additionally, free FPIX exerts strong oxidative stress on lipid membranes like the digestive vacuole of the parasite. As *Plasmodium* does not have other pathways of FPIX detoxification,[13] free FPIX can lead to membrane destruction and death of the parasite. The presence of CQ and DioC may thereby lead to stronger association of FPIX to the membrane and thus increases its toxic effect to the *Plasmodium* parasites. However, interference with other enzymatic pathways can not be ruled out. Most likely, antimalarial activity of both drugs is the result of both modes of action.

Conclusions

We have presented the first structural model of the complex formed between ferriprotoporphyrin IX heme and the novel antimalarial compound DioC, derived from the measurement of NMR paramagnetic relaxation. DioC associates with FPIX in a similar manner as found for other antimalarial drugs. The drug molecule is likely to be stabilized by a water molecule coordinated to the iron in FPIX. This structural feature may help in

the development of novel antimalarial compounds of the NIQ class.

Acknowledgements

This work was supported by the Deutsche Forschungsgemeinschaft (SFB 630 "Novel Agents against Infectious Diseases", projects A2 and C2). K.F.S. acknowledges a fellowship and G.B. supplies from the Fonds der Chemischen Industrie. We thank Dr. Matthias Grüne for making spectrometer time available.

Keywords: heme · malaria · naphthylisoquinoline alkaloid · NMR spectroscopy · paramagnetic relaxation

[1] R. W. Snow, C. A. Guerra, A. M. Noor, H. Y. Myint, S. I. Hay, *Nature* **2005**, *434*, 214 – 217.
[2] M. Foley, L. Tilley, *Int. J. Parasitol.* **1997**, *27*, 231 – 240.
[3] R. F. Loeb, W. M. Clarke, G. R. Coateney, L. T. Coggeshall, F. R. Dieuaide, A. R. Dochez, E. G. Hakansson, E. K. Marshall, S. C. Marvel, O. R. McCoy, J. J. Sapero, W. H. Serbell, J. A. Shannon, G. A. Carden, *J. Am. Med. Assoc.* **1946**, *130*, 1069 – 1070.
[4] P. Schlagenhauf, A. Tschopp, R. Johnson, H. D. Nothdurft, B. Beck, E. Schwartz, M. Herold, B. Krebs, O. Veit, R. Allwinn, R. Steffen, *J. Inclusion Phenom. Macrocyclic Chem.* **2003**, *327*, 1078 – 1081.
[5] M. Foley, L. Tilley, *Pharmacol. Ther.* **1998**, *79*, 55 – 87.
[6] World Health Organization, *International travel and health 2005*, WHO, Geneva, **2005**.
[7] S. Pagola, P. W. Stephens, D. S. Bohle, A. D. Kosar, S. K. Madsen, *Nature* **2000**, *404*, 307 – 310.
[8] L. Cheng, J. Lee, D. R. Powell, G. B. Richter-Addo, *Acta Crystallogr. Sect. E* **2004**, *60*, M1340 – M1342.
[9] J. Silver, B. Lukas, *Inorg. Chim. Acta* **1983**, *78*, 219 – 224.
[10] A. Chai, R. Chevli, C. Fitch, *Biochemistry* **1980**, *19*, 1543 – 1549.
[11] C. R. Chonga, D. J. Sullivan, Jr., *Biochem. Pharmacol.* **2003**, *66*, 2201 – 2212.
[12] T. J. Egan, K. K. Ncokazi, *J. Inorg. Biochem.* **2005**, *99*, 1532 – 1539.
[13] P. Loria, S. Miller, M. Foley, L. Tilley, *Biochem. J.* **1999**, *339*, 363 – 370.
[14] L. M. B. Ursos, P. D. Roepe, *Med. Res. Rev.* **2002**, *22*, 465 – 491.
[15] M. J. Dascombe, M. G. B. Drew, H. Morris, P. Wilairat, S. Auparakkitanon, W. A. Moule, S. Alizadeh-Shekalgourabi, P. G. Evans, M. Lloyd, A. M. Dyas, P. Carr, F. M. D. Ismail, *J. Med. Chem.* **2005**, *48*, 5423 – 5436.
[16] T. J. Egan, *Drug Des. Rev.–Online* **2004**, *1*, 93 – 110.
[17] T. J. Egan, *J. Inorg. Biochem.* **2006**, *100*, 916 – 926.
[18] A. Leed, K. DuBay, L. M. B. Ursos, D. Sears, A. C. de Dios, P. D. Roepe, *Biochemistry* **2002**, *41*, 10245 – 10255.
[19] L. Banci, I. Bertini, G. Cavallaro, A. Giachetti, C. Luchinat, G. Parigi, *J. Biomol. NMR* **2004**, *28*, 249 – 261.
[20] L. Bertini, C. Luchinat, G. Parigi, *Prog. Nucl. Magn. Reson. Spectrosc.* **2002**, *40*, 249 – 273.
[21] A. C. de Dios, L. B. Casabianca, A. Kosar, P. D. Roepe, *Inorg. Chem.* **2004**, *43*, 8078 – 8084.
[22] A. C. de Dios, R. Tycko, L. M. B. Ursos, P. D. Roepe, *J. Phys. Chem. A* **2003**, *107*, 5821 – 5825.
[23] G. Bringmann, M. Rübenacker, R. Weirich, L. Aké Assi, *Phytochemistry* **1992**, *31*, 4019 – 4024.
[24] G. Bringmann, *From tropical lianas to novel antiplasmodial agents: The naphthylisoquinoline alkaloids*, World Health Organisation, Geneva, **2003**.
[25] G. François, G. Timperman, W. Eling, L. Aké Assi, J. Holenz, G. Bringmann, *Antimicrob. Agents Chemother.* **1997**, *41*, 2533 – 2539.
[26] I. Bertini, C. Luchinat, G. Parigi, *Solution NMR of Paramagnetic Molecules*, Elsevier, New York, **2001**.
[27] G. N. La Mar, W. D. J. Horrocks, *NMR of Paramagnetic Molecules: Principles and Applications*, Academic Press, New York, **1973**.
[28] I. Solomon, *Phys. Rev.* **1955**, *99*, 559 – 565.
[29] D. F. Evans, *J. Am. Chem. Soc.* **1959**, *81*, 2003 – 2005.
[30] J. L. Deutsch, S. M. Poling, *J. Chem. Educ.* **1969**, *46*, 167 – 168.
[31] P. Maccarthy, *Anal. Chem.* **1978**, *50*, 2165 – 2165.
[32] K. Hirose, *J. Inclusion Phenom. Macrocyclic Chem.* **2001**, *39*, 193 – 209.
[33] R. M. Theisen, J. Shearer, W. Kaminsky, J. A. Kovacs, *Inorg. Chem.* **2004**, *43*, 7682 – 7690.
[34] M. L. Liu, X. A. Mao, C. H. Ye, H. Huang, J. K. Nicholson, J. C. Lindon, *J. Magn. Reson.* **1998**, *132*, 125 – 129.
[35] C. D. Schwieters, J. J. Kuszewski, N. Tjandra, G. M. Clore, *J. Magn. Reson.* **2003**, *160*, 65 – 73.
[36] G. J. Kleywegt, T. A. Jones, *Acta Crystallogr. Sect. D* **1998**, *54*, 1119 – 1131.
[37] G. J. Kleywegt, K. Henrick, E. J. Dodson, D. M. F. van Aalten, *Structure* **2003**, *11*, 1051 – 1059.
[38] W. L. DeLano, *The PyMOL Molecular Graphics System*, DeLano Scientific, San Carlos, CA, **2002**.
[39] M. Nilges, *J. Mol. Biol.* **1995**, *245*, 645 – 660.
[40] I. Constantinidis, J. D. Satterlee, *J. Am. Chem. Soc.* **1988**, *110*, 927 – 932.
[41] S. Tsuzuki, K. Honda, T. Uchimaru, M. Mikami, K. Tanabe, *J. Am. Chem. Soc.* **2002**, *124*, 104 – 112.
[42] S. Moreau, B. Perly, J. Biguet, *Biochimie* **1982**, *64*, 1015 – 1025.
[43] V. A. Pashynska, H. Van den Heuvel, M. Claeys, *J. Am. Soc. Mass Spectrom.* **2004**, *15*, 1181 – 1190.
[44] T. Frosch, B. Kustner, S. Schlucker, A. Szeghalmi, M. Schmitt, W. Kiefer, J. Popp, *J. Raman Spectrosc.* **2004**, *35*, 819 – 821.
[45] S. R. Vippagunta, A. Dorn, H. Matile, A. K. Bhattacharjee, J. M. Karle, W. Y. Ellis, R. G. Ridley, J. L. Vennerstrom, *J. Med. Chem.* **1999**, *42*, 4630 – 4639.
[46] T. J. Egan, W. W. Mavuso, D. C. Ross, H. M. Marques, *J. Inorg. Biochem.* **1997**, *68*, 137 – 145.
[47] T. J. Egan, K. K. Ncokazi, *J. Inorg. Biochem.* **2004**, *98*, 144 – 152.
[48] M. M. Maltempo, *J. Chem. Phys.* **1974**, *61*, 2540 – 2547.
[49] N. Stiefl, G. Bringmann, C. Rummey, K. Baumann, *J. Comput.-Aided Mol. Des.* **2003**, *17*, 347 – 365.

Received: November 7, 2006
Revised: December 19, 2006
Published online on February 21, 2007

